

Modeling the effects of nonlinear equilibrium sorption on the transport of solute plumes in saturated heterogeneous porous media

A. Abulaban *, J.L. Nieber

Department of Biosystems and Agricultural Engineering, University of Minnesota, St. Paul and Army High Performance Computing Research Center, University of Minnesota, Minneapolis, USA

Abstract

Transport of sorbing solutes in 2D steady and heterogeneous flow fields is modeled using a particle tracking random walk technique. The solute is injected as an instantaneous pulse over a finite area. Cases of linear and Freundlich sorption isotherms are considered. Local pore velocity and mechanical dispersion are used to describe the solute transport mechanisms at the local scale. This paper addresses the impact of the degree of heterogeneity and correlation lengths of the log-hydraulic conductivity field as well as negative correlation between the log-hydraulic conductivity field and the log-sorption affinity field on the behavior of the plume of a sorbing chemical. Behavior of the plume is quantified in terms of longitudinal spatial moments: center-of-mass displacement, variance, 95% range, and skewness. The range appears to be a better measure of the spread in the plumes with Freundlich sorption because of plume asymmetry. It has been found that the range varied linearly with the travelled distance, regardless of the sorption isotherm. This linear relationship is important for extrapolation of results to predict behavior beyond simulated times and distances. It was observed that the flow domain heterogeneity slightly enhanced the spreading of nonlinearly sorbing solutes in comparison to that which occurred for the homogeneous flow domain, whereas the spreading enhancement in the case of linear sorption was much more pronounced. In the case of Freundlich sorption, this enhancement led to further deceleration of the solute plume movement as a result of increased retardation coefficients produced by smaller concentrations. It was also observed that, except for plumes with linear sorption, correlation between the hydraulic conductivity and the sorption affinity fields had minimal effect on the spatial moments of solute plumes with nonlinear sorption. © 2000 Elsevier Science Ltd. All rights reserved.

Keywords: Solute transport; Porous media; Equilibrium sorption; Freundlich isotherm; Particle tracking random walk; Retardation

1. Introduction

The transport equation of a sorbing chemical involves several hydraulic and chemical parameters that can be spatially and/or temporally variable in natural subsurface environments. Detailed evaluation of such parameters at every point in a flow field is cost prohibitive, if at all possible, no matter how small the domain may be. However, such variability plays a primary role in the behavior of a chemical plume migrating in such domains.

Due to the random spatial variability of natural porous formations, stochastic methods for handling parameter fields have been more popular among researchers in this field [1,11,12,18,16,30,45,47]. The stochastic approach of simulation of groundwater flow and

transport assumes that the hydrogeologic parameters are random functions in space (random fields) that can be fully characterized by their statistical moments. In the computational area of stochastic analysis, numerical experiments are carried out on hypothetical flow fields with specified statistics for the hydrogeologic parameters being examined [2,6,11–13,18–21,33,34,40,41,47]. Among the computational methods used in stochastic analysis, one of the major developments has been the application of the random walk technique for modeling solute transport in heterogeneous porous media in a computationally efficient manner [27,47,50].

In a previous paper, the authors examined the behavior of nonlinearly sorbing solutes in a homogeneous saturated flow field [4]. This paper presents simulation results using the particle tracking random walk (PTRW) technique to analyze the transport of substances with nonlinear equilibrium sorption in 2D heterogeneous saturated porous media. Heterogeneity of the porous medium is assumed to be structured, with known

* Corresponding author.

probability distributions and covariance functions. Emphasis will be placed on the effects of randomly distributed hydraulic conductivity and sorption affinity parameters on the development of plumes of nonlinearly sorbing solutes. Related studies have been reported by Tompson [48], who performed 3D simulations on a 25 m cube, and Bosma and van der Zee [8], who did 2D simulations on continuously injected solutes. In both of those studies, however, only a single Freundlich isotherm was considered and they both focused on the first two spatial moments of the solute plume. In addition to the Freundlich isotherm, Tompson [48] also considered a case with Langmuir isotherm. More recently, Bosma et al. [9] considered multiple Freundlich isotherms using Monte Carlo simulations to predict average plume behavior in terms of the first two spatial moments.

The objective of this paper is to examine the sensitivity of plume behavior to the Freundlich isotherm in the presence of physical and chemical heterogeneities in the transport medium. Evaluation is carried out in terms of longitudinal spatial moments, namely mean displacement, spread variance, and plume skewness.

2. The transport model

The transport of a sorbing chemical can be described by the advection–dispersion–sorption equation

$$\frac{\partial C}{\partial t} + \nabla \cdot (C\mathbf{v}) - \nabla \cdot (\mathbb{D} \cdot \nabla C) + \frac{\rho}{\Phi} \frac{\partial S}{\partial t} = 0, \quad (1)$$

where C is the concentration in the liquid phase [ML^{-3}]; S the concentration in the sorbed phase expressed as mass of solute per unit mass of solid [M/M]; \mathbf{v} the local velocity vector [LT^{-1}]; ρ the dry bulk density of the porous matrix [ML^{-3}]; Φ the effective porosity [L^3/L^3]; and t is time [T]. The hydrodynamic dispersion tensor, \mathbb{D} [L^2T^{-1}] is defined as

$$\mathbb{D} = (\alpha_T V + D_m)\mathbf{I} + (\alpha_L - \alpha_T) \frac{\mathbf{v}\mathbf{v}}{V}, \quad (2)$$

where D_m is the molecular diffusion coefficient [L^2T^{-1}]; \mathbf{I} the identity matrix; V the magnitude of the velocity vector, α_L and α_T are the longitudinal and transverse dispersivities [L], respectively; and $\mathbf{v}\mathbf{v}$ is the diadic of the velocity vector.

Using the identity $\nabla \cdot (\mathbb{D} \cdot \nabla C) = \nabla \nabla : (\mathbb{D}C) + (\nabla C) \cdot (\nabla \cdot \mathbb{D})$, and rearranging terms, Eq. (1) above can be rewritten in terms of the total solute concentration and in a form analogous to the Fokker–Planck equation as (see also [47] and [4] for details)

$$\begin{aligned} \frac{\partial \Phi C_T}{\partial t} + \nabla \cdot \left(\frac{\mathbf{v}(\mathbf{x}, t) + \nabla \cdot \mathbb{D}(\mathbf{x}, t)}{R(C, \mathbf{x})} \Phi C_T \right) \\ - \nabla \nabla : \left(\frac{\mathbb{D}(\mathbf{x}, t)}{R(C, \mathbf{x})} \Phi C_T \right) = 0, \end{aligned} \quad (3)$$

where C_T is the total mass concentration expressed as mass of solute per unit liquid volume [ML^{-3}], and is defined as

$$C_T = C + \frac{\rho(\mathbf{x})}{\Phi(\mathbf{x})} S \quad (4)$$

and the function $R(C, \mathbf{x})$ is defined as

$$R(C, \mathbf{x}) = 1 + \frac{\rho(\mathbf{x})}{\Phi(\mathbf{x})} \frac{S}{C}, \quad (5)$$

which is a concentration- and space-dependent retardation coefficient.

We should note here that there is an issue related to the existence of the spatial derivatives in the discrete form of Eq. (3). If C , \mathbf{v} and \mathbb{D} are all at least twice differentiable, the spatial derivatives in both Eqs. (1) and (3) will be defined. If we use a finite difference scheme, with a piecewise constant representation for C , \mathbf{v} and \mathbb{D} , the spatial derivatives will be defined in Eq. (1), whereas for this same level of representation, the spatial derivatives in Eq. (3) will be undefined. In our analysis, we use a particle method with the Langevin stepping equation [4] to solve Eq. (3), rather than using a direct finite difference discretization. In the stepping equation, the only spatial derivative is the term $\nabla \cdot \mathbb{D}(\mathbf{x}, t)$. This derivative is approximated at cell centers with a forward or backward difference scheme, but it is not defined at the interfaces of computational elements. However, the derivatives at an element interface are approximated as the average of the derivatives at the centers of the elements on both sides of the interface. While we recognize the strict mathematical problem associated with existence of derivatives in Eq. (3), the form of Eq. (3) is the one used in all the previous applications of the Fokker–Planck equation to solute transport in porous media [4,8,9,47,48]. The issue about the existence of the spatial derivatives in the discrete form of Eq. (3) is outside the scope of this study and will have to be addressed in a later analysis.

Introducing the variables $\mathbf{v}_r(\mathbf{x}, t, C) = (\mathbf{v} + \nabla \cdot \mathbb{D})/R(C, \mathbf{x})$ and $\mathbb{D}_r(\mathbf{x}, t, C) = \mathbb{D}/R(C, \mathbf{x})$, which are the *retarded* (or effective) velocity and dispersion tensor, respectively, and assuming that the porosity is constant, Eq. (3) can be rewritten as

$$\frac{\partial C_T}{\partial t} + \nabla \cdot [\mathbf{v}_r(\mathbf{x}, t, C) C_T] - \nabla \nabla : [\mathbb{D}_r(\mathbf{x}, t, C) C_T] = 0. \quad (6)$$

The transport equation above will be subject to the widely used Freundlich isotherm expressed as

$$S(C, \mathbf{x}) = K_f(\mathbf{x}) C^n, \quad (7)$$

where $K_f(\mathbf{x})$ [L^3M^{-1}] n is the sorption affinity and n is the Freundlich exponent. The retardation coefficient thus becomes

$$R(C, \mathbf{x}) = 1 + \frac{\rho(\mathbf{x})}{\phi} K_f(\mathbf{x}) C^{n-1}. \quad (8)$$

The value of the Freundlich exponent n depends on the chemical properties of both the solute and the porous medium. It has been observed to be generally less than 1.0, but there have been a few exceptions where it was reported to be slightly larger than 1.0 [23]. The parameter K_f is also a function of the chemical characteristics of the sorbent and sorbate (solid matrix), as well as the environment in the system. For a given chemical constituent, the magnitude of K_f is influenced by such factors as the availability of sorption sites (surface area of the porous medium), organic content, mineral composition of the porous medium, the presence of other ions competing for the same sorption sites, temperature, and pH of the system, to name only a few [17,23,26,35,36,38,39,43,52].

The variability of the sorption affinity is a significant factor in the distribution of sorbing solutes in groundwater. However, literature on the natural variability of the sorption affinity is scarce. Jackson and Inch [25] studied the behavior of ^{90}Sr in a heterogeneous porous media. They investigated the effects of the variability of the sorption affinity on the distribution of ^{90}Sr . They found that ... “the principal factor affecting the distribution of ^{90}Sr is the spatial variability in the adsorption affinity of the aquifer materials as measured by the specific surface area of the aquifer sediments. Effects of ionic competition between ^{90}Sr and other ions (Ca^{2+} , stable Sr^{2+} , H^+) were less important”. Heterogeneity was also observed in the sorption affinity in the Borden site experiment [31].

In this work, it will be assumed that the limiting factor affecting the variability of the sorption affinity parameter is the availability of sorption sites. Availability of sorption sites depends on the specific surface area of the porous medium, which is a function of the granular size of the aquifer material. The finer the sediments, the larger the specific surface area and thus the larger the sorption affinity. Experimental evidence to support this hypothesis is limited. Direct evidence is given by Jackson and Inch [25], which was quoted above. Through his work on the adsorption capability of activated carbon, Kulkarni [28] showed that equilibrium concentrations of solute in the fluid phase in a solution of activated carbon and water were smaller for finer carbon particles, and also that equilibrium was attained faster.

It is well documented that the hydraulic conductivity is a function of the size of the sediment particles [14]. Through the dependence of both sorption affinity and hydraulic conductivity on the size of sediment particles, correlation can be derived between the hydraulic conductivity and the sorption affinity. Assuming hydraulic conductivity to be related to particle size alone for

spherical particles, Abulaban [3] and Garabedian et al. [15] showed theoretically negative correlation between the logarithm of the sorption affinity and the logarithm of the hydraulic conductivity and found the proportionality constant for the derived correlation to be $-\frac{1}{2}$. Negative correlation between retardation characteristics of porous media and flow velocity was assumed by Valocchi [51] and has been observed by Hess et al. [24]. Negative correlation between surface area and permeability has also been discussed in several more recent studies [5,10,37,42,49].

In the present analysis, the hydraulic conductivity, K (L/T), and thus the sorption affinity coefficient, are assumed to be log-normally distributed in space. This means that if $Y = \ln(K/K_G)$, and $W = \ln(K_f/K_{fG})$, where K_G and K_{fG} are the geometric means of the hydraulic conductivity and the sorption affinity coefficient, respectively, then Y and W will be normally distributed. Correlation between $\ln K$ and $\ln K_f$, means that Y can be written in terms of W using the following stochastic relationship:

$$W = \beta Y + \epsilon, \quad (9)$$

where β is the proportionality constant and ϵ is a zero-mean error whose variability is much smaller than that of W , i.e., $\sigma_\epsilon \ll \sigma_W$, and is introduced to account for imperfect correlation between Y and W .

In two related studies [9,54], perfect correlation was assumed and β was chosen to be -1.0 . The basis for selecting this value of β was that this led to perfect correlation between Y and W . However, this is an incorrect premise because β is not a measure of the degree of correlation, but only a scaling between the variables. Perfect correlation exists when $\text{cov}(Y, W)/\sqrt{\sigma_Y \sigma_W} = \pm 1.0$, which occurs for any nonzero value of β if and only if ϵ is constant, not only if $\beta = \pm 1.0$.

The negative correlation between hydraulic conductivity and sorption affinity must be understood in terms of their influence on the effective velocity of the solute. Solute effective velocity is the flow velocity scaled by the retardation coefficient. The larger the sorption affinity, the larger the retardation. Therefore, in a high conductivity zone, the flow velocity will be large, and since the sorption affinity will be small, retardation will also be small (but larger than 1.0), and hence the effective velocity will not be much smaller than the flow velocity. Conversely, in a low conductivity zone the flow velocity will be small. Due to the negative correlation with the hydraulic conductivity, sorption affinity will be large, and therefore the retardation coefficient will be large, producing a retarded velocity that is significantly smaller than the flow velocity. Depending on the magnitudes of flow velocities, this behavior may produce larger variations among the retarded velocities and hence enhance plume spreading.

3. Flow and transport problem

The transport problem considered here involves a 2D flow domain with mean flow along the principal axis of the flow domain. The flow domain is described in our previous paper [4]. The hydraulic conductivity field is generated using the turning bands method [32,46]. The log-hydraulic conductivity field is assumed to be isotropic with an exponential auto-covariance function. Log-hydraulic conductivity fields were generated for four values of $\sigma_{\ln K}$: 0.25, 0.5, 0.75, and 1.0; and two correlation lengths, $\lambda_{\ln K}$, of 5 and 10 m. It should be noted that the fields corresponding to the same correlation length were all generated from one realization of the random field and this realization was scaled for the desired standard deviation. This was done to produce similar fields with peaks and valleys in the same locations so that we avoid variabilities caused by different initial behavior of the plume, since we are dealing with a nonlinear sorption process that is sensitive to plume characteristics at early times.

The sorption affinity field was transformed from the hydraulic conductivity field using the proportionality constant of -0.5 . Simple analysis shows that $\sigma_{\ln K_r} = |\beta|\sigma_{\ln K}$, and thus the standard deviations of the log-sorption affinity fields corresponding to those of the log-conductivity field were 0.125, 0.25, 0.375, and 0.5. The correlation lengths are the same however. The geometric means of the hydraulic conductivity field was 10 m/d. The geometric mean of the sorption affinity field was $2 \times 10^{-7} \text{ (l/mg)}^n$. Matrix bulk density was 1.75 g/ml and porosity was 0.35, both of which were assumed to be constant. Longitudinal and transverse dispersivities were 0.1 and 0.02 m, respectively. The flow domain was discretized into 1 m square elements. The flow field corresponds to a mean hydraulic gradient of -0.035 which results in a mean pore velocity of 1.0 m/d for the constant effective porosity of 0.35 used in the simulations. The flow fields corresponding to these conditions were solved using the finite element method.

The transport problem consists of releasing 200 g of a sorbing chemical uniformly distributed over a $50 \text{ m} \times 10 \text{ m}$ rectangular area aligned with the direction of the mean flow. Since the total mass is constant, there is a different initial liquid concentration for each Freundlich exponent (see [4] for details). The solute mass is represented with 10^6 particles of constant mass. Our approach is based on a single realization to observe the large time behavior of the solute plume.

4. Results and discussion

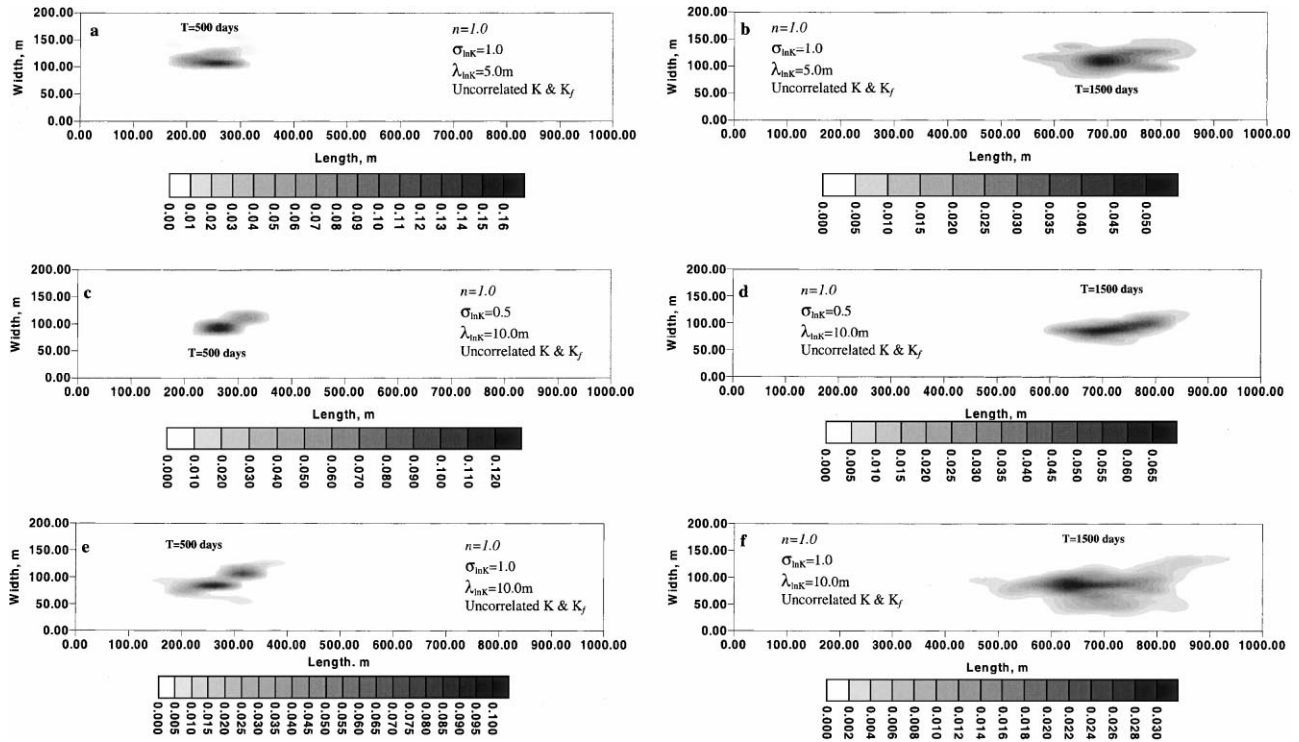
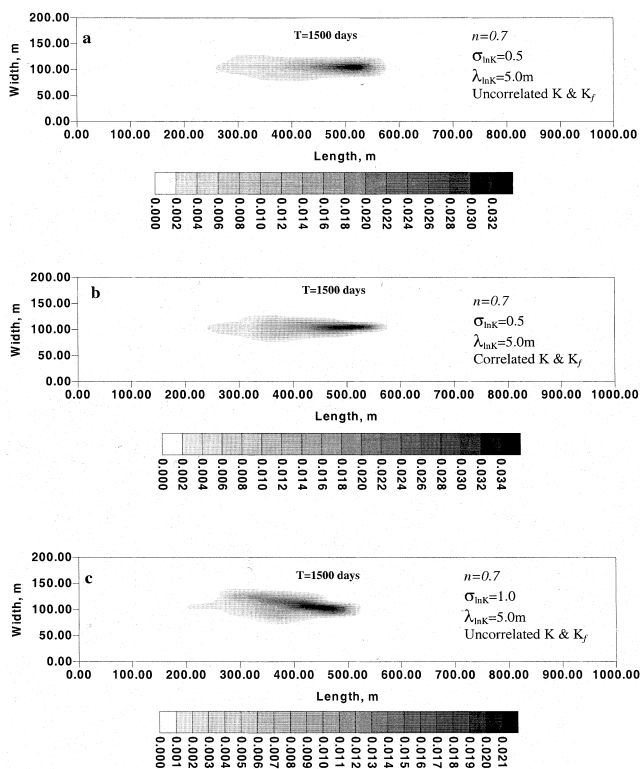
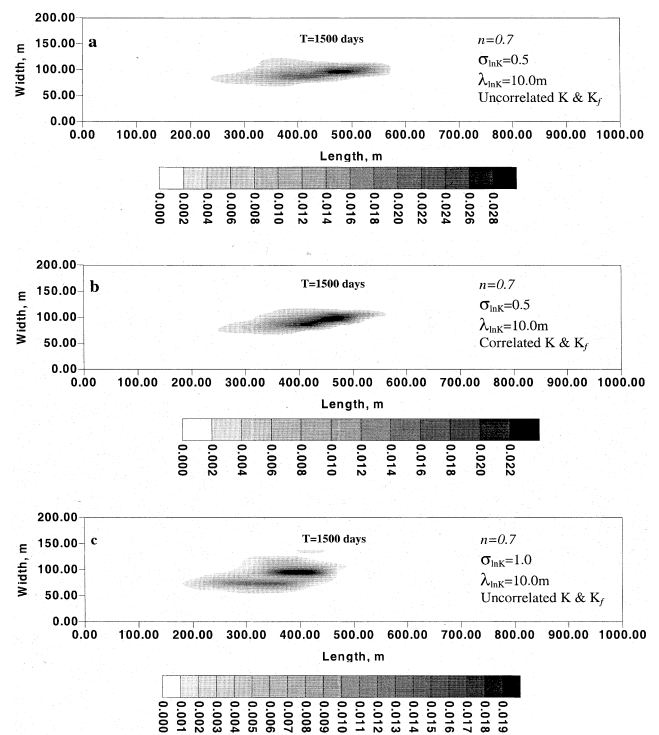
Results of the simulations are presented here in terms of concentration distributions, center of mass displacement, spread variance, and skewness. Due to the pro-

nounced asymmetry of the plumes it is thought that the variance is a poor measure of spatial spread, so the 95% range, μ_{95} , is also presented as an alternative measure of spatial spread. The range is defined as the distance within which 95% of the solute mass is contained. Its lower and upper bounds are the 2.5 and 97.5 percentile of the solute mass, respectively. All the spatial moments are calculated for the liquid mass concentration. Results for all of these measures are presented along with those for the homogeneous flow field for comparison.

4.1. Concentration profiles

Total concentrations, C_T , are calculated from the particle distribution by taking the total mass of particles in a computational element and dividing it by the pore volume. The liquid concentration is calculated from the total concentration by numerically solving a nonlinear equation to partition the total mass in an element between the liquid and sorbed phases [4]. Sample concentration plumes are depicted in Figs. 1–5. The distributions shown in Fig. 1(a–f) are sample concentration plumes for the linear isotherm case for different combinations of the log-hydraulic conductivity standard deviation (hereafter referred to as standard deviation) and correlation length. Among these there are plumes that manifest breakup early in the plume development (plumes c and e). Plots of the velocity fields corresponding to those cases (not shown) showed that the initial plume size was very small relative to the scale of velocity field variations, making the plume very susceptible to changes in the velocity field. The breakup was more pronounced in the cases shown in Fig. 1 than in the cases not shown because in these cases either the standard deviation or the correlation length (or both) was large, affecting the magnitude of the velocity variations as well as the size of coherent velocity zones. It should be noted here that the effects of the breakup of the plume were still present even after large times, where one would expect the plume to become contiguous due to the mixing process it has undergone.

Shown in Fig. 2 are sample concentration plumes for $n = 0.7$ after 1500 d for the correlation length of 5 m, and in Fig. 3 are some distributions for the correlation length of 10 m. It is interesting to see that the trailing edge is wider than the leading front, which was not observed to occur for the case of homogeneous flow fields [4]. The mechanism that causes the wide tail is the same mechanism responsible for the stretching of the tail of the plume discussed by Abulaban et al. [4]. At the inception of the plume when the concentrations are large and the retardation coefficients are small, the retarded velocities and dispersion coefficients are relatively large, causing the plume to spread in both the longitudinal and transverse directions at a relatively high rate. This spreading is enhanced by the local velocity gradients

Fig. 1. Sample concentration distributions for the Freundlich exponent $n = 1.0$.Fig. 2. Sample concentration distributions for the Freundlich exponent $n = 0.7$ and a log-hydraulic conductivity field correlation length of 5 m.Fig. 3. Sample concentration distributions for the Freundlich exponent $n = 0.7$ and a log-hydraulic conductivity field correlation length of 10 m.

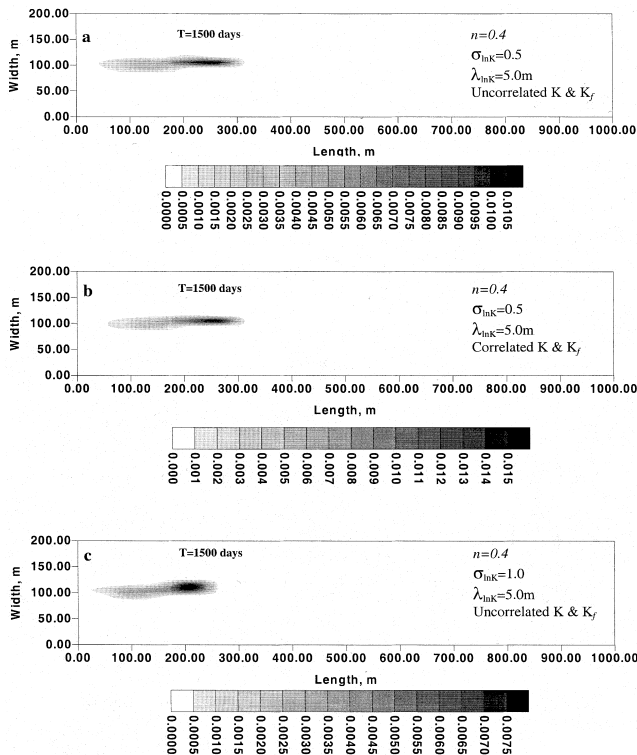


Fig. 4. Sample concentration distributions for the Freundlich exponent $n = 0.4$ and a log-hydraulic conductivity field correlation length of 5 m.

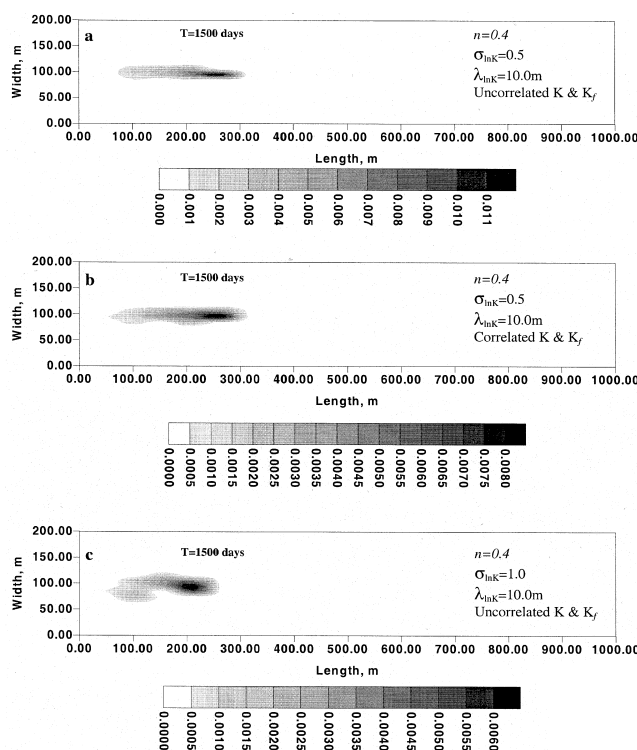


Fig. 5. Sample concentration distributions for the Freundlich exponent $n = 0.4$ and a log-hydraulic conductivity field correlation length of 10 m.

caused by the heterogeneity in the hydraulic conductivity field. Along the trailing edge the large retardation coefficients associated with the small concentrations prevent the solute from receding, thereby producing the wide tail. However, the large retardation on the periphery of the leading front hinders the spreading in the transverse direction.

As we can see from Figs. 2(b) and 3(b), correlation in the hydraulic conductivity and sorption affinity fields enhance the narrowing of the leading front of the plume. This behavior affects the calculated longitudinal spatial moments, especially the higher order ones (variance and skewness), because these are determined by the longitudinal distribution of the solute. It is apparent from the plumes in Figs. 2(c) and 3(c) where the standard deviation is the largest that these plumes experienced breakup.

The sample concentration plumes for the Freundlich exponent of 0.4 are shown in Fig. 4 for the correlation length of 5 m and in Fig. 5 for the correlation length of 10 m. The first thing to notice in those two plumes is that they are the narrowest and the slowest, as one would expect since the retardation coefficients are the largest for this case. It can also be seen that the leading front has the tendency to become narrower, but because the plumes have not travelled large distances, the narrower fronts are not readily obvious. Again, the plumes for the largest standard deviation depicted in Figs. 4(c) and 5(c) show that the plume experienced breakup with the largest breakup occurring for the case of the larger correlation length. Note that because the plumes are very slow, it takes a very long time for them to completely develop into the typical shape of a spreading solute plume. Simulations with $n = 0.4$ were run to about 96,000 d and it was found that the plumes travelled less than 600 m and the center-of-mass velocities dropped to about 0.001 m/d.

4.2. Center-of-mass displacement

It was found that the hydraulic conductivity field with the smallest standard deviation (0.25) had minimal effect on the center-of-mass displacement for both correlation lengths (not shown) as compared to the homogeneous case. This behavior is in agreement with the abundant literature addressing the effects of parameter heterogeneity on the flow field [1,12,45,47]. Due to this observation we decided to present results for the two larger standard deviations, 0.5 and 1.0. The displacement of the plume center-of-mass is depicted in Fig. 6 for those two standard deviations and for the correlation length of 5 m. The general behavior of the curves shown in Fig. 6 is similar to that of the homogeneous flow field with the slope decreasing as the exponent n decreases. Variations from the homogeneous case grow as the standard deviation increases. Also the curves for the different

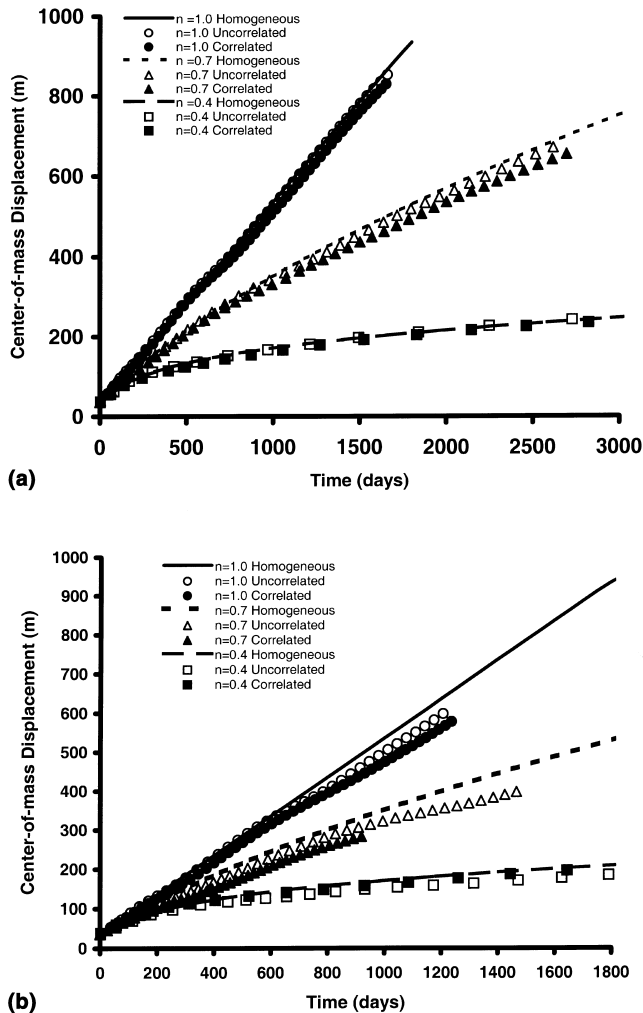


Fig. 6. Distance travelled by the center-of-mass for the correlation length of 5 m and (a) $\ln(K)$ std. dev. = 0.5, and (b) $\ln(K)$ std. dev. = 1.0.

isotherms coincide with those for the homogeneous cases up to 200 d or more, depending on the heterogeneity of the flow field. This is because the solute is initially uniformly distributed and the concentrations are relatively large, producing retardation coefficients that are very close to 1.0.

It appears from Fig. 6(a) that the correlation between the hydraulic conductivity and the sorption affinity had very little effect on the behavior of the plume displacement. This was the case for all the levels of heterogeneity and correlation lengths considered. This is because the process of nonlinear sorption dominates over the correlation in that the concentration dependence of the retardation coefficient prevails over the sorption affinity coefficient. This leads to the conclusion that the levels of variability considered here for the sorption affinity coefficient are insignificant in the course of plume development. In other words, negligible errors would have resulted if the sorption affinity fields were treated as being homogeneous.

For the case of the larger standard deviation (Fig. 6(b)), the plume spreading is enhanced and concentrations decrease. Since the retardation increases with decreasing concentrations, it is seen that the plume velocity, represented by the slope of the displacement curves, decreases. Note how the curves for the strongest isotherm nonlinearity of $n = 0.4$ tend to level off much faster than the case for the weaker nonlinearity of $n = 0.7$. It is interesting to see that at about 600 d the displacement curve for the case of the heterogeneous flow with the linear isotherm falls below the displacement curve for the homogeneous case and does not seem to rebound back. This behavior can be attributed to the persistence of the flow field caused by the spatial correlation in the hydraulic conductivity field. Close examination of the curve for the same case towards the end of the simulation reveals that it has started to tend back to join with the curve for the homogeneous case.

The effects of the larger correlation length on the plume displacement are illustrated in Fig. 7. It is clear that deviations from the homogeneous case are greater for this case. The deceleration of growth of the displacement is greater compared to the case for the smaller correlation length, especially for the case corresponding to the larger standard deviation. The curves for the heterogeneous cases for the three different isotherms for the larger standard deviation (Fig. 7(b)) all show a speedup early on, up to about 400 d, followed by a slow down. This indicates the presence of a high conductivity zone downgradient of the injection area. The faster deceleration of the plume in these cases results because of the larger spread (slight though it may be) of the solute plume, and is consistent with the effects of the correlation length and the standard deviation of the log-hydraulic conductivity on the flow field reported in the literature [1,12,45,47]. The effect of the correlation length on the deceleration of the displacement appears to be greater for the case of $n = 0.7$ than for both cases of $n = 0.4$ and $n = 1.0$. This happens because for $n = 1.0$ the rate of spreading is independent of the magnitude of the concentration, and for $n = 0.4$ the plume moves so slowly that it does not spread as quickly as the case for $n = 0.7$.

4.3. Spatial spread moments

Another spatial moment considered for our study is the longitudinal spread variance shown in Figs. 8 and 9. Note that the curves are plotted against the displacement of the center-of-mass and not against time, which is done to compare the behavior of the plumes in terms of the distance travelled since the plume velocities are not uniform.

Compared to the homogeneous cases, the influence of flow field heterogeneity on the plume variance of the nonlinearly sorbing chemicals is insignificant, even for

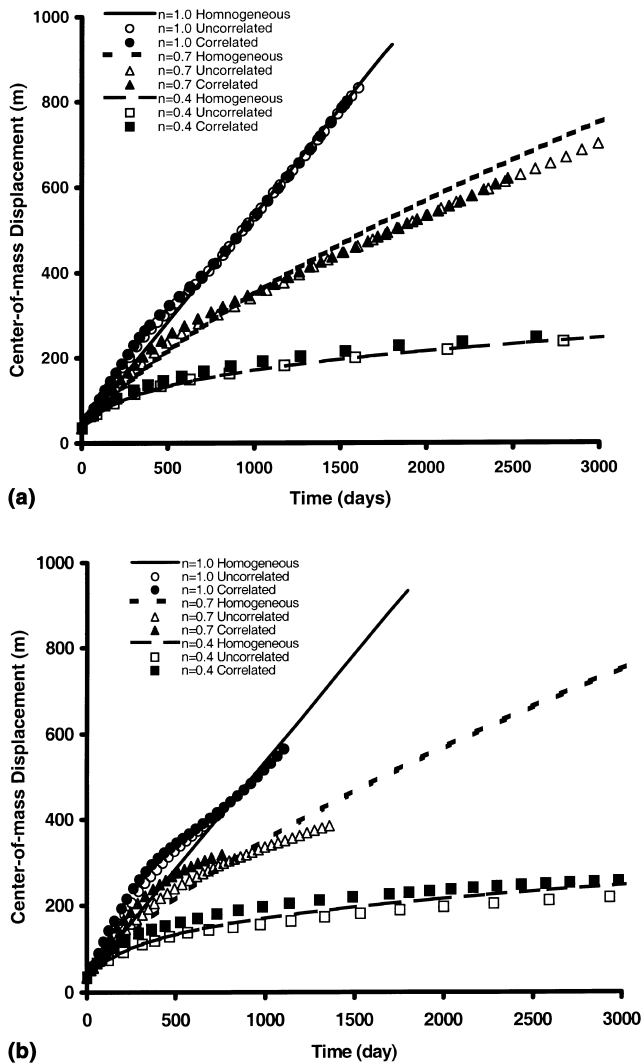


Fig. 7. Distance travelled by the center-of-mass for the correlation length of 5 m and (a) $\ln(K)$ std. dev. = 0.5, and (b) $\ln(K)$ std. dev. = 1.0.

the largest heterogeneity considered here. In terms of the Freundlich exponent, the influence is the least for the case with the strongest nonlinearity. This is because the greater the nonlinearity, the slower the plume becomes and therefore the smaller the area traversed by it, resulting in less heterogeneity of the flow field experienced by the plume. Similar behavior was also observed by Bosma et al. [9] and Srivastava and Brusseau [44]. This behavior is in line with the findings reported in the literature that plume broadening due to dispersion increases as the square root of the travelled distance, whereas that due to “nonlinear” sorption increases linearly with the distance travelled [7,22,29]. The behavior of the curves for $n = 0.7$ depicted in Fig. 8(b) is however peculiar. The wide spread between the curves for the correlated and uncorrelated fields is most likely due to the presence of a zone of high velocity contrast, as is also obvious from the curves for the linear isotherm.

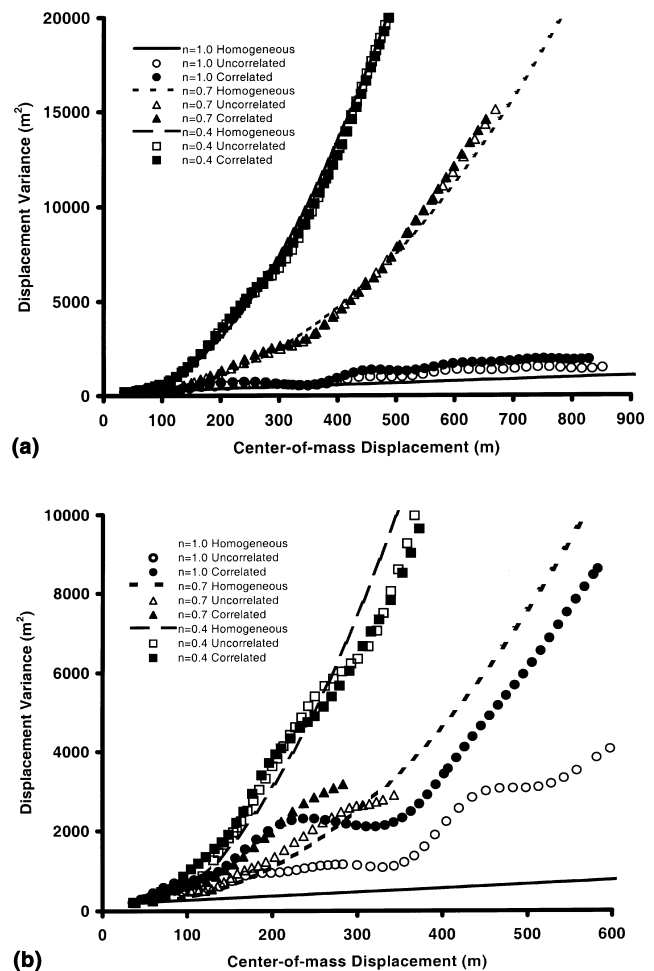


Fig. 8. Spatial variance vs travelled distance for the correlation length of 5 m and (a) $\ln(K)$ std. dev. = 0.5, and (b) $\ln(K)$ std. dev. = 1.0.

However, the situation is different for the linear isotherm case. The presence of variability in the hydraulic conductivity field has a pronounced effect on the spreading of the plume, which effect increases with increasing the standard deviation or the correlation length or both. This effect has been well documented in the literature [1,12,45,47]. For the case of the largest standard deviation and correlation length (Fig. 9(b)) the effect of the heterogeneity on the spatial variance of the linear case is so great that the variance cannot be distinguished from that of the nonlinear case with $n = 0.7$. This implies that if such a variance was observed in the field, it would not be possible to tell whether it was due to flow field heterogeneity or nonlinear sorption. Similar behavior was also reported in another study [44].

Contrary to the case with the nonlinear isotherms the correlation between the hydraulic conductivity and the sorption affinity plays a significant role in the development of the plume for the case of linear sorption. As can be seen from Figs. 8 and 9, the effect of the correlation grows with the correlation length. It can also be seen from the plots that the effect of cross-correlation be-

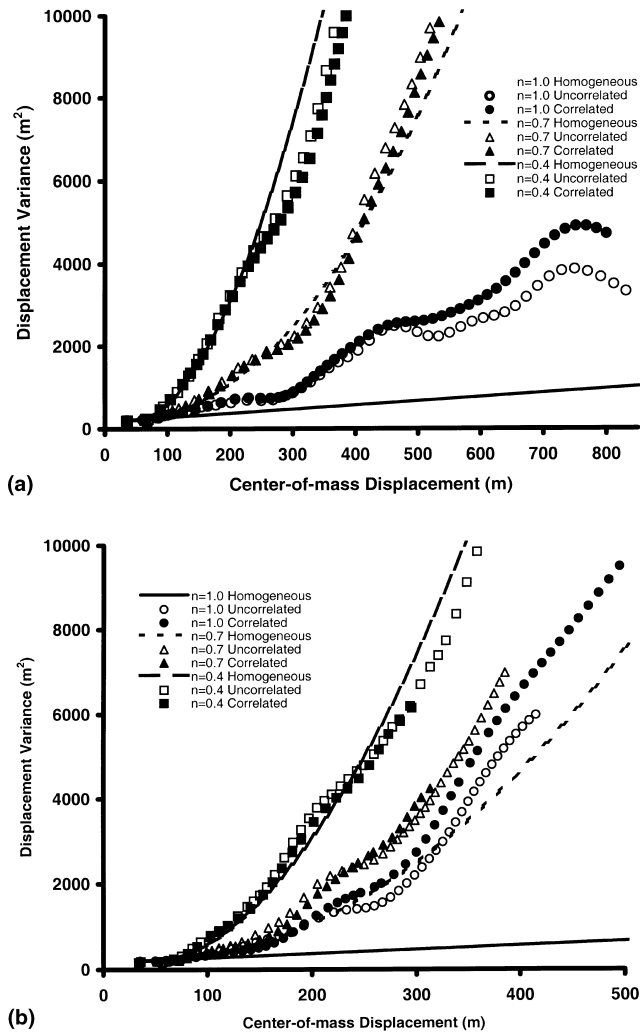


Fig. 9. Spatial variance vs travelled distance for the correlation length of 10 m and (a) $\ln(K)$ std. dev. = 1.0, and (b) $\ln(K)$ std. dev. = 1.0.

tween the two fields grows with the standard deviation. This is because the retardation coefficient depends only on the variable sorption affinity coefficient and not on the concentration. As discussed above, negative correlation between the hydraulic conductivity and the sorption affinity coefficient widens the relative variations among the retarded velocities, and this enhances the spreading relative to the uncorrelated case. This is seen here because of the absence of concentration dependence of the retardation coefficient, which dependence was seen to dominate the behavior of plumes with nonlinear sorption.

Due to the asymmetry of the solute plumes undergoing nonlinear sorption, the variance is deemed to be a poor measure of spatial spread. Sometimes the variance for an asymmetric distribution can be larger than for another one that appears to be wider [53]. We propose that a more intuitive and robust measure of the spatial spread is the range of the distribution. In our analysis, we chose to look at the 95% range as an alternative

measure of spatial spread. The 95% range, μ_{95} , is defined as the distance between the 2.5 and the 97.5 percentile of the solute mass.

The 95% range curves are shown in Figs. 10 and 11. The range is a more well-behaving function than the variance in that it is more representative of the spatial spread of the plume. As was discussed in our previous paper [4], the nonlinear sorption process is a counter dispersive one in that it acts against the spreading of the plume front and the nonlinearly increasing variance is due to the stretching tail, which has larger weight in the calculation of the variance. We also discussed that because of the self-sharpening effect of the nonlinear sorption process the plume is expected to reach a point where the front stops spreading and that the stretching of the tail would be the primary cause of the increasing variance. In fact this was shown to be the case in our

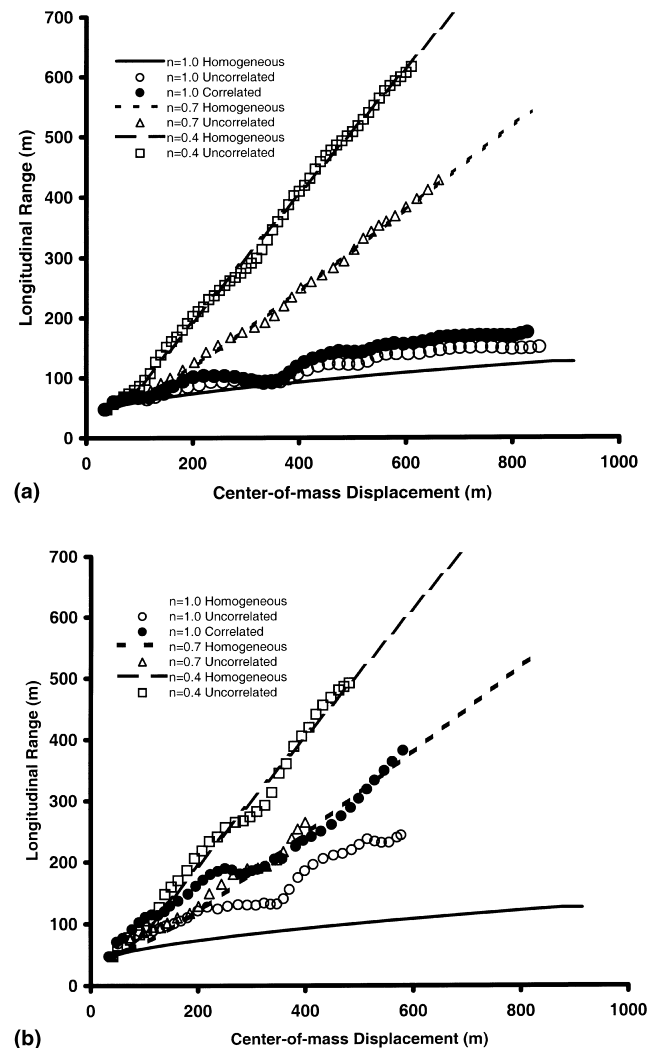


Fig. 10. 95% Longitudinal range vs travelled distance for the correlation length of 5 m and (a) $\ln(K)$ std. dev. = 0.5, and (b) $\ln(K)$ std. dev. = 1.0.

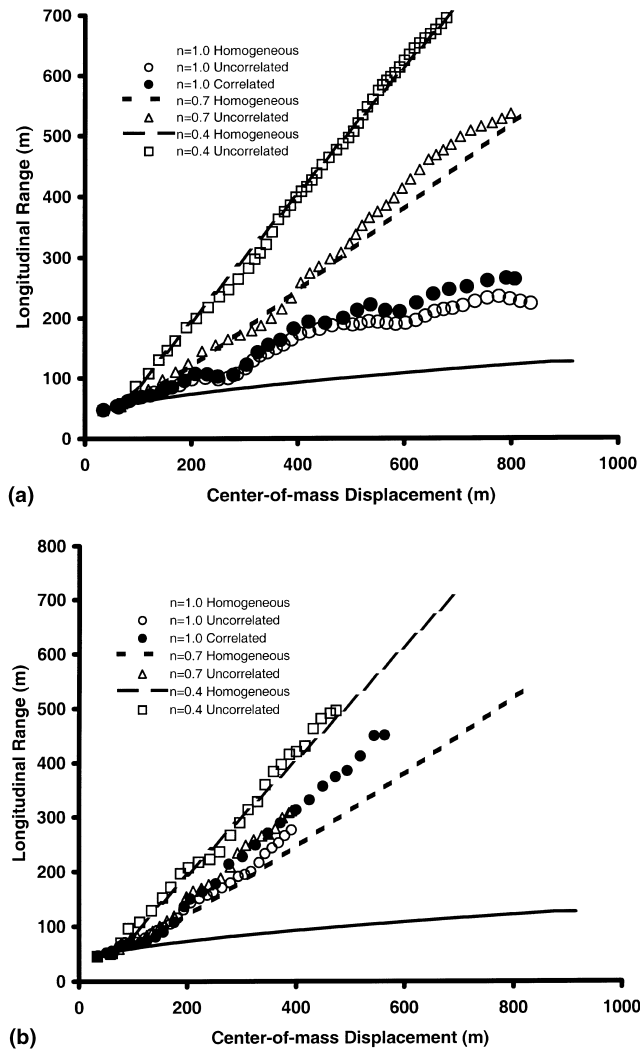


Fig. 11. 95% Longitudinal range vs travelled distance for the correlation length of 10 m and (a) $\ln(K)$ std. dev. = 0.5, and (b) $\ln(K)$ std. dev. = 1.0.

earlier manuscript by the linear behavior of the center of mass-to-peak curves showing the distance between the center-of-mass and the location of the peak concentration. By examining the behavior of the 95% range for the nonlinear cases, we can clearly see that the spreading behavior of the plume is more accurately represented by this statistic. The fact that the plots of the range for the nonlinear isotherms are virtually linear attests to the foregoing argument. The behavior of the linear isotherm is consistent with that observed earlier from the variance plots.

Examining the difference between the curves for the homogeneous and the heterogeneous cases for spatial variance as well as for the range corresponding to a particular Freundlich exponent, we can see that the curves are virtually coincident for $n = 0.4$ and that there is a small gap in the case of $n = 0.7$. The gap is larger for the linear case, however, and it grows with distance

travelled. This suggests that there must be some Freundlich exponent at which flow field heterogeneity becomes more dominant than isotherm nonlinearity in the plume spatial behavior. The nonlinear increase of the gap between the corresponding heterogeneous and homogeneous curves, and the high sensitivity of the plume spread to a slight nonlinearity in the Freundlich exponent suggest that such an exponent would be very close to 1.0. Note that in Figs. 10 and 11 only the curves for the uncorrelated hydraulic conductivity and sorption affinity fields were shown for the cases with nonlinear sorption. The curves for the correlated fields lay almost on top of the curves for the uncorrelated cases, and that is why they were omitted. The fact that the curves for the correlated and uncorrelated fields lay on top of each other attests to the argument presented above in the discussion about the spread variance, that correlation in the parameter fields had little effect on the behavior of solute plumes with nonlinear sorption.

The fact that the curves for all the three isotherms and, by interpolation, for any isotherm in between, are linear is very important for extrapolation purposes, which is a very important objective for doing modeling studies. From linear trends one can extrapolate quantities beyond the limit of simulated times and distances, whereas extrapolation from nonlinear trends, such as the variance, would be difficult and highly inaccurate, at best.

4.4. Plume skewness

The last spatial moment considered for analysis is the third central moment, skewness, shown in Figs. 12 and 13. Again, we chose to show the curves for the cases with no cross-correlation between the hydraulic conductivity and the sorption affinity fields because those showed similar behavior with no additional information gained from the fact that parameter fields were correlated. First, it should be noted that all the curves had a positive trend early on in the simulations. This is because initially the concentrations are large and uniformly distributed, and thus the retardation coefficients are uniformly distributed. This means that at the start of a simulation, dispersive effects are significant, producing the flatter fronts that cause the positive skewness. Shortly after that, the skewness curves for the nonlinear sorption cases fall to the negative region. It is readily seen from the graphs that oscillations from the homogeneous cases become wider as the standard deviation increases.

It is also readily seen from Figs. 12 and 13 that for both correlation lengths, the curves for the milder standard deviation of 0.5 tend to approach the curves for the homogeneous cases after “sufficiently” large distances travelled. Deviations from the homogeneous cases are largest for the larger standard deviation, and they are equally large in the cases of linear and nonlinear

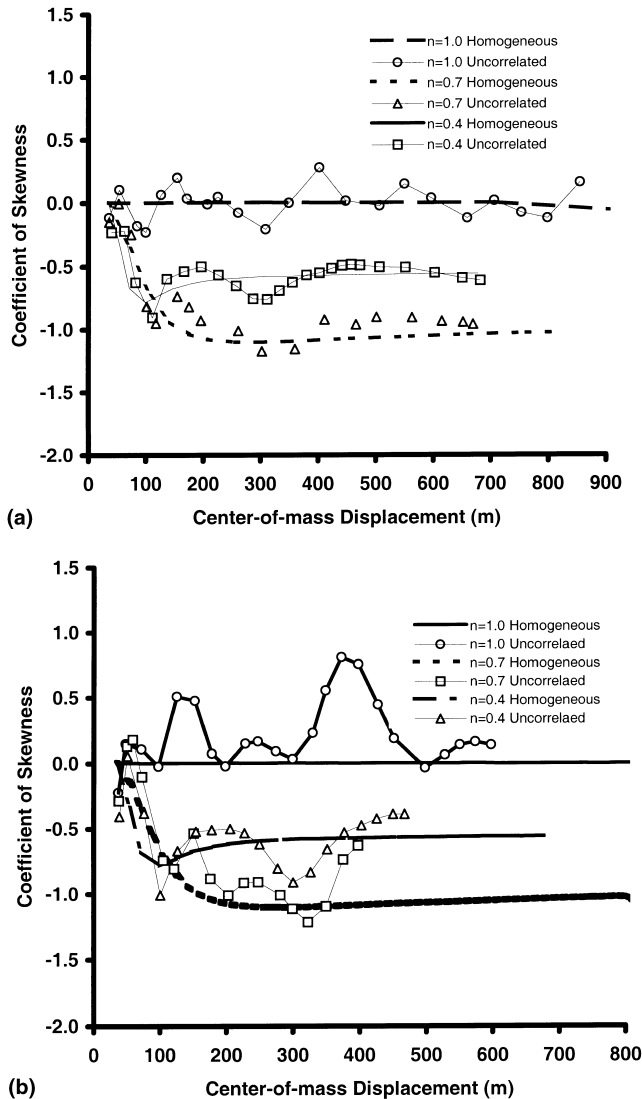


Fig. 12. Skewness coefficient vs travelled distance for the correlation length of 5 m and (a) $\ln(K)$ std. dev. = 0.5, and (b) $\ln(K)$ std. dev. = 1.0.

sorption, even though the curves for the smaller correlation length have started to show signs of their tendency to approach the curves for the homogeneous cases. The magnitude of fluctuations might be reduced by starting with a much larger plume that samples larger areas of the flow velocity variations, thus making it less susceptible to small scale heterogeneities as far as the spatial moments are concerned. Results for the correlated hydraulic conductivity and sorption affinity fields (not shown) showed very similar behavior to those with no cross-correlation.

While we saw that the flow field heterogeneity had very small effect on the solute plumes with $n \neq 1.0$ in terms of the spatial variance and range, its impact on the plume skewness is quite evident. The reason for this is that among the spatial moments analyzed, skewness is the most sensitive to irregularities in the shape of the

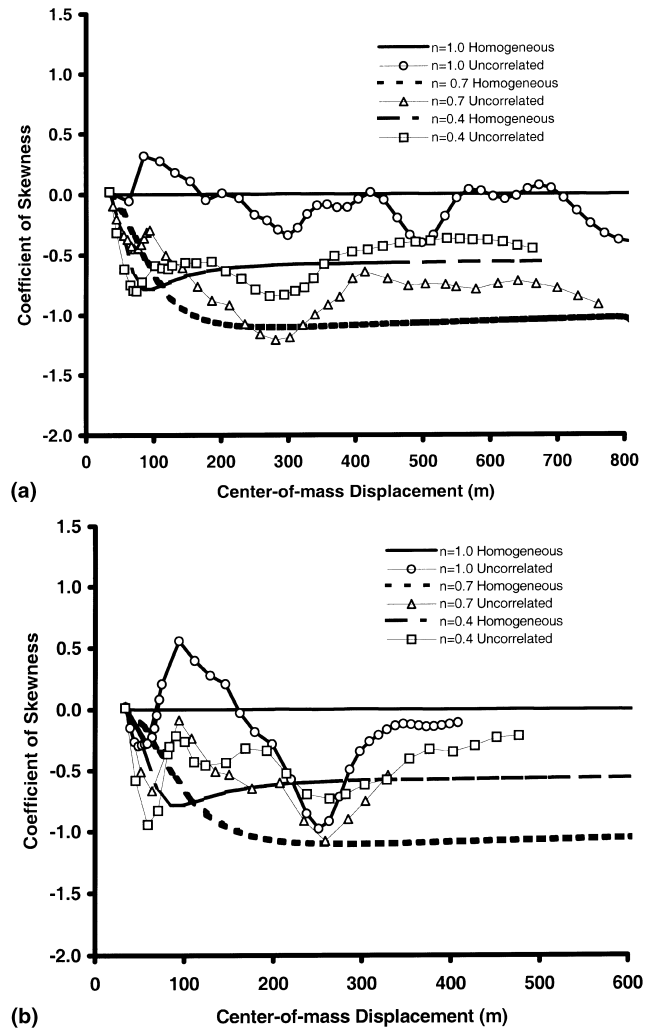


Fig. 13. Skewness coefficient vs travelled distance for the correlation length of 10 m and (a) $\ln(K)$ std. dev. = 0.5, and (b) $\ln(K)$ std. dev. = 1.0.

plume. This is also why we saw from Figs. 12 and 13 that the skewness coefficient in all cases considered started to tend to approach the curves for the homogeneous cases after the plumes became fairly large, at which times the flow field starts to look to the plume as if it were homogeneous.

5. Summary and conclusions

The work presented in this paper was a continuation to an earlier endeavor by the authors, which analyzed the plume behavior for nonlinearly sorbing chemicals in saturated homogeneous porous media. In this paper, we analyzed the behavior of such chemicals in physically and chemically heterogeneous saturated flow fields. Two scenarios were considered in terms of correlation between hydraulic conductivity and sorption affinity fields: uncorrelated and perfectly correlated with a

proportionality constant of -0.5 . The simulations involved the release of 200 g of a solute represented by 10^6 particles that were tracked in the flow field using a particle tracking random walk method. Results were presented in terms of concentration distributions and spatial moments of the plumes: center of mass, variance, 95% range, and skewness. The results for homogeneous flow fields were also shown for comparison.

Compared to the homogeneous fields, flow field heterogeneities caused more spreading of the solutes, which resulted in larger retardation in the cases of nonlinear sorption and therefore relatively slower plumes. For the three log-hydraulic conductivity standard deviations of 0.25, 0.5, and 1.0, and the two correlation lengths of 5 and 10 m that were considered, the mechanism of nonlinear sorption seemed to prevail over the effects of flow field heterogeneity. Correlation between the hydraulic conductivity and sorption affinity fields did not affect the results in terms of spatial moments for the nonlinear sorption scenarios either. In contrast, for those two factors, flow field heterogeneity and correlation, significant effects were observed on the behavior of the plumes with linear sorption because of the independence of the retardation coefficient on the magnitude of the solute concentration.

While the curves for the spatial spread variance were highly nonlinear for the cases of nonlinear sorption, the curves for the 95% range for both linear and nonlinear sorption were linear. Linear trends have a practical advantage for extrapolation beyond the limits of the times and distances examined in the simulations, while extrapolation from nonlinear trends is difficult and not very accurate, if at all possible.

Due to the small size of the initial solute plumes relative to the scale of velocity field heterogeneities, it was observed that in the cases of the larger heterogeneities the plumes were broken up at the beginning of the simulations. This caused the spatial moments to oscillate erratically around the values of the moments derived for the homogeneous flow fields. Oscillatory behavior was especially prevalent for skewness since it is the moment most sensitive to any irregularity in the *solute* distribution.

Acknowledgements

Published as Paper No. 001120039 of the scientific journal series of the Minnesota Agricultural Experiment Station on research conducted under Minnesota Agricultural Experiment Station Project No. 12-047. This work was also supported by the Army High Performance Computing Research Center under the auspices of the Department of the Army, Army Research Laboratory cooperative agreement number DAAH04-95-2-0003/contract number DAAH04-95-C-0008, the

content of which does not necessarily reflect the position or the policy of the government, and no official endorsement should be inferred. CRAY time for numerical simulations was provided in part by the Supercomputer Institute at the University of Minnesota.

References

- [1] Ababou R, McLaughlin D, Gelhar LW, Tompson AFB. Numerical simulation of three-dimensional saturated flow in randomly heterogeneous porous media. *Transp Porous Media* 1989;4:549.
- [2] Ababou R, Gelhar LW. Self-similar randomness and spectral conditioning: Analysis of scale effects in subsurface hydrology. In: Cushman JH, editor. *Dynamics of fluids in hierarchical porous media*, San Diego, CA: Academic Press, 1990.
- [3] Abulaban A. Modeling the transport of sorbing solutes in heterogeneous porous media. Ph.D. Dissertation, Department of Civil and Mineral Engineering, Minnesota: University of Minnesota, Minneapolis, 1993.
- [4] Abulaban A, Nieber JL, Misra D. Modeling the transport of nonlinearly sorbing solutes in saturated homogeneous porous media. *Adv Water Resour* 1998;21(6):487–96.
- [5] Allen-King RM, Halket RM, Gaylord DR, Robin MJL. Characterizing the heterogeneity and correlation of perchloroethene sorption and hydraulic conductivity using a facies-based approach. *Water Resour Res* 1998;34(3):385–96.
- [6] Bakr AA, Gelhar LW, Gutjahr AL, MacMillan JR. Stochastic analysis of variability in subsurface flows, 1. Comparison of one- and three-dimensional flows. *Water Resour Res* 1978;14:263–72.
- [7] Bolt GH. Movement of solutes in soils: principles of adsorption/exchange chromatography. In: Bolt GH, editor. *Soil chemistry B physico-chemical models*, second ed. Amsterdam: Elsevier, 1982. p. 285–348.
- [8] Bosma WJP, van der Zee SEATM. Dispersion of a continuously injected, nonlinearly adsorbing solute in chemically or physically heterogeneous porous formations. *J Cont Hydrology* 1995;18: 181–98.
- [9] Bosma WJP, van der Zee SEATM, van Duijn CJ. Plume development of a nonlinearly adsorbing solute plume in heterogeneous porous media. *Water Resour Res* 1996;32:1569–84.
- [10] Burr DT, Sudicky EA, Naff RL. Nonreactive and reactive solute transport in three-dimensional heterogeneous porous media: mean displacement, plume spreading, and uncertainty. *Water Resour Res* 1994;30(3):791–816.
- [11] Dagan G. Solute transport in heterogeneous porous formations. *J Fluid Mech* 1984;145:151–77.
- [12] Dagan G. Statistical theory of groundwater flow and transport: pore to laboratory, laboratory to formation, and formation to regional scale. *Water Resour Res* 1986;22:120S–34S.
- [13] Freeze RA. A stochastic-conceptual analysis of one-dimensional flow in nonuniform homogeneous media. *Water Resour Res* 1975;11:725–41.
- [14] Freeze RA, Cherry JA. *Groundwater*, Englewood Cliffs, NJ: Prentice-Hall, 1979. p. 604.
- [15] Garabedian SP, Gelhar LW, Celia MA. Large scale dispersive transport in aquifers: field experiment and reactive transport theory, Report # 315, Ralph Parsons Laboratory, Department of Civil Engineering, Cambridge, MA: MIT Press, 1988.
- [16] Garabedian SP, LeBlond DR, Gelhar LW, Celia MA. Large-scale natural gradient tracer test in sand and gravel aquifer, Cape Cod, Massachusetts, 2. Analysis of spatial moments for nonreactive tracer. *Water Resour Res* 1991;27:910–24.
- [17] Gasser RPH. *An introduction to chemisorption and catalysis by metals*. New York: Oxford University Press, 1985. p. 260.

- [18] Gelhar LW. Stochastic analysis of flow in heterogeneous porous media. In: Bear J, Corapcioglu M, editors. *Fundamentals of transport phenomena in porous media*. Dordrecht: Martinus Nijhof, 1984. p. 673–717.
- [19] Gelhar LW. Stochastic theory of transport in saturated and unsaturated porous media. In: Bear J, Corapcioglu M, editors. *Advances of transport in porous media*. Dordrecht: Martinus Nijhof, 1987. p. 657.
- [20] Gelhar LW, Axness CW. Three-dimensional analysis of macrodispersion in aquifers. *Water Resour Res* 1983;19:161–80.
- [21] Graham W, McLaughlin D. Stochastic analysis of nonstationary subsurface solute transport, 1. Unconditional moments. *Water Resour Res* 1989;25:215–32.
- [22] Griffioen J, Appelo CAJ, van Veldhuizen M. Practice of chromatography: deriving isotherms from elution curves. *Soil Sci Soc Am J* 1992;56:1429–37.
- [23] Hamaker JW, Thompson JM. Adsorption. In: Goring CM, Hamaker JW, editors. *Organic chemicals in the soil environment*. New York: Marcel-Dekker, 1972.
- [24] Hess KM, Davis JA, Fuller CC, Coston JA. Spatial variability of metal-ion adsorption in a glacial outwash aquifer, AGU Spring Meeting, Abstract, EOS, Trans Am Geophysical Union, Baltimore, MD, 1993.
- [25] Jackson RE, Inch JK. The in situ adsorption of ^{90}Sr in a sand aquifer at the Chalk River Nuclear Laboratories. *J Cont Hydrology* 1989;4:27–50.
- [26] Karickhoff SW. Organic pollutants in aquatic systems. *J Hydraulic Eng* 1984;110:707–35.
- [27] Kinzelbach W. The random walk method in pollutant transport simulation. In: Custodio E, Gurgui A, Lobo Ferreira JP, editors. *Groundwater flow and transport modeling D*. Dordrecht: Riedel, 1988.
- [28] Kulkarni SR. Modification of a mathematical model to take into account particle size distribution in fixed bed carbon adsorption systems, MS Thesis, Department of Civil Engineering, Manhattan: Kansas State University, 1983.
- [29] Lai SH, Jurinak JJ. Cation adsorption in one-dimensional flow through soils: a numerical solution. *Water Resour Res* 1972;8:99–107.
- [30] LeBlanc DR, Garabedian SP, Hess KM, Gelhar LW, Quadri RD, Stollenwerk KG, Wood WW. Large-scale natural gradient tracer test in sand and gravel aquifer, Cape Cod. Massachusetts, 1. Experimental design and observed tracer movement. *Water Resour Res* 1991;27:895–910.
- [31] Mackay DM, Ball WP, Durant MG. Variability of aquifer sorption properties in a field experiment on groundwater transport of organic solutes: methods and preliminary results. *J Cont. Hydrology* 1986;1:119–32.
- [32] Mantoglou A, Wilson JL. The turning bands method for the simulation of random fields using line generation by a spectral method. *Water Resour Res* 1982;18:1379–94.
- [33] Mantoglou A, Gelhar LW. Stochastic modeling of large scale, transient unsaturated flow systems. *Water Resour Res* 1987;23:37–46.
- [34] Neuman SP, Winter CL, Newman CM. Stochastic theory of field scale dispersion in anisotropic porous media. *Water Resour Res* 1987;23:453.
- [35] Nkedi-Kizza P, Rao PSC, Hornsby AG. Influence of organic cosolvents on sorption of hydrophobic organic chemicals by soils. *Environ Sci Technol* 1985;19:975–9.
- [36] Piwoni M, Banerjee P. Sorption of volatile organic solvents from aqueous solution onto subsurface solids. *J Cont Hydrology* 1989;4:163–179.
- [37] Rajaram H. Time and scale dependent effective retardation factors in heterogeneous aquifers. *Adv Water Resour* 1997;20(4):217–30.
- [38] Rao PS, Jessup RE. Sorption and movement of pesticides and other toxic organic substances in soils. In: Nelson DW, Elrick DE, Tanji KK, editors. *Chemical mobility and reactivity in soil systems*, Proceedings of a symposium sponsored by divisions S-1, S-2 and A-5 of the American Society of Agronomy and the Soil Science Society of America in Atlanta, GA, 29 November–3 December, 1981, SSSA special pub. # 1983;11.
- [39] Schwarzenbach RP, Westall J. Transport of nonpolar organic components from surface water to groundwater: laboratory sorption studies. *Environ Sci Technol* 1981;15:1360–7.
- [40] Smith L, Freeze RA. Stochastic analysis of steady state groundwater flow in a bounded domain, 1. One-dimensional simulations. *Water Resour Res* 1979a;15:521–8.
- [41] Smith L, Freeze RA. Stochastic analysis of steady state groundwater flow in a bounded domain, 2. Two-dimensional simulations. *Water Resour Res* 1979b;15:1543–59.
- [42] Smith L. Theoretical relationships between reactivity and permeability for monomineralic porous media, Materials Research Society Symposia Proceedings, Materials Research Society, Pittsburgh, PA, 1996;412:693–700.
- [43] Sposito G. *The surface chemistry of soils*. New York: Oxford University Press, 1984. p. 234.
- [44] Srivastava R, Brusseau ML. Nonideal transport of reactive solutes in heterogeneous porous media: 1. Numerical model development and moments analysis. *J Cont Hydrology* 1996;24:117–43.
- [45] Sudicky EA. A natural gradient experiment on solute transport in a sandy aquifer: spatial variance of hydraulic conductivity and its role in the dispersion process. *Water Resour Res* 1986;22:2069–82.
- [46] Tompson AFB, Vomvoris EA, Gelhar LW. Numerical simulation of solute transport in randomly heterogeneous porous media: motivation, model development and application, Rep. #36, Ralph M. Parson Laboratory, Department of Civil Engineering, Mass Institute of Technology, Cambridge, MA, 1988.
- [47] Tompson AFB, Gelhar LW. Numerical simulation of solute transport in three-dimensional randomly heterogeneous porous media. *Water Resour Res* 1990;26:2541–62.
- [48] Tompson AFB. Numerical simulation of chemical migration in physically and chemically heterogeneous porous media. *Water Resour Res* 1993;29:3709–26.
- [49] Tompson AFB, Jackson, Reactive transport in heterogeneous systems: an overview, Reviews in Mineralogy, Mineralogical Society of America 1996;34.
- [50] Uffink GJM. A random walk method for the simulation of macrodispersion in a stratified aquifer. In: Dunin FX, Matthess G, Gras RA, editors. *Relation of groundwater quality and quantity*, Proceedings IUGG–IAHS Symposium in Hamburg, vol. 146. Oxfordshire, Wallingford: IAHS, 1985. p. 103–14.
- [51] Valocchi AJ. Spatial moment analysis of the transport of kinetically adsorbing solutes. *Water Resour Res* 1989;25:273–80.
- [52] Weber WJ, Jr., McGinley PM, Katz LE. Sorption phenomena in subsurface systems: concepts, models, and effects on contaminant fate and transport. *Water Res* 1991;25:499–528.
- [53] Wilson BN. Bayesian estimation of erosion parameters, Part I: theoretical development. *Trans Am Soc Agri Eng* 1991;34:809–20.
- [54] Yang J, Zhang R, Wu J, Allen MB. Stochastic analysis of adsorbing solute transport in two-dimensional unsaturated soils. *Water Resour Res* 1996;32:2747–56.